Behaviour of Offshore Structures Conference (BOSS'92), London, Great Britain, 1992.

Mean yaw moment on floating bodies advancing with a forward speed in waves

John Grue and Enok Palm

Department of Mathematics, Mechanics Division,
University of Oslo

Abstract

The mean yaw moment acting on a turret production ship (TPS) and a tension-leg platform (TLP) advancing with a small speed in waves is studied. Special emphasis is paid to the contribution from steady second order velocities in the fluid, which in the formulae for the moment are multiplied with the forward speed. This contribution is found to amount to 30-100% of the forward speed part of the moment when the wave period is larger than $9 - 10s$. Largest effect occurs, surprisingly, when the wave direction is orthogonal to the forward speed direction. Also the effect of an irregular sea is discussed.

1 Introduction

In a recent paper (Grue and Palm 1992) formulae were derived for the steady second order forces and moments acting on a floating body advancing with a forward speed U in waves. The formulae were derived using the near field method, i.e. pressure integration over the body, as well as using the far field method, based on conservation of linear and angular momentum. Obviously the expressions for the mean second order forces and moments contain terms being proportional to products of two first order quantities. It turned out, however, that using the near field method all the derived formulae for the forces and moments also possessed terms depending on the steady second order velocity field, the $\psi^{(2)}$-field. Applying the far field procedure, also the formulae for the steady vertical moment, the mean drift yaw moment, contained terms depending on the $\psi^{(2)}$-field whereas the horizontal forces did not contain such terms, provided that the velocity circulation in the fluid vanishes. To obtain the steady drift yaw moment it is therefore not sufficient to know the first order field. We also have to solve for the steady second order velocity. It was shown in the above mentioned paper how this can be performed for small values of the forward speed. It was, however, also shown how the contribution from the $\psi^{(2)}$-field to the yaw drift moment may be obtained for small U-values without solving for $\psi^{(2)}$.

In the present paper we first review shortly the theoretical background. The main intention is, however, to use the derived formulae to evaluate the steady yaw moment acting on a turret production ship (TPS) and a tension-leg platform (TLP). The yaw moment is computed for various values of the incident wave angle, with special emphasis on the importance of the $\psi^{(2)}$-field.

The complete formula for the mean yaw moment is given by (19) where the last term is due to the $\psi^{(2)}$-field. We notice that the yaw moment is here totally determined by the knowledge of the first order motion. The computations show that the largest contributions from the $\psi^{(2)}$-field is obtained for incoming waves propagating orthogonal to the forward speed direction. Furthermore, we find for the TPS (with length $L = 230m$) and the TLP (with column radius $a = 10m$), that the peak value of the $\psi^{(2)}$-contribution occurs when the wave period is between $10s$ and $15s$. Hence, the peak value of the contribution from $\psi^{(2)}$ is found for wave periods where the wave spectrum often has its maximal value, which leads to a substantial contribution from the $\psi^{(2)}$-field to the mean yaw moment. The mean yaw moment is also computed for an irregular sea, to further illustrate the effect of the $\psi^{(2)}$-field.

2 Theory

2.1 The steady yaw moment

We consider a marine structure moving horizontally with constant speed U and responding to long-crested incoming waves with small amplitude. U is assumed small, such that terms being quadratic or of higher order in U may be neglected. A frame of reference $O - xyz$ moving with forward speed U in the same direction as the structure is introduced. The xy-plane is in the undisturbed free surface, the x-axis in the direction of the forward motion, and the z-axis positive upwards. Unit vectors $\mathbf{i},\mathbf{j},\mathbf{k}$ are introduced respectively along the x, y, z-directions. It is assumed that the motion is irrotational and the fluid incompressible. The total fluid velocity may then be written

$$\mathbf{v} = \nabla\Phi + U\nabla\chi_s \tag{1}$$

Here χ_s is the steady velocity potential generated by the moving structure, independent of the incoming waves, and Φ is the velocity potential due to incoming, scattered and radiated waves. χ_s and Φ both satisfy the Laplace equation. χ_s may be decomposed by $\chi_s = -x + \chi$, where $-x$ represents the uniform current potential (due to the forward translation) and χ the steady disturbance due to the structure. χ behaves like a dipole far away from the structure. Φ may be written

$$\Phi = \phi^{(1)} + \phi^{(2)} + \psi^{(2)} \tag{2}$$

where $\phi^{(1)}$ is the linear oscillatory potential proportional to the wave amplitude, and $\phi^{(2)}$ and $\psi^{(2)}$ are the oscillatory and steady second order potentials proportional to the wave amplitude squared, respectively.

The steady yaw moment with respect to $\mathbf{x} = (x, y, z) = 0$ acting on the marine structure may be obtained from the flux of angular momentum at a vertical circular cylinder S_∞ in the far field, i.e.

$$M_z = -\mathbf{k} \cdot \overline{\int_{S_\infty} (p\mathbf{x} \times \mathbf{n} + \rho\mathbf{x} \times \mathbf{v}\mathbf{v} \cdot \mathbf{n}) dS} \tag{3}$$

Here a bar denotes the time average, p pressure, ρ fluid density and $v_n = \mathbf{v} \cdot \mathbf{n}$. $\mathbf{n}$ denotes the normal vector, positive out of the fluid. Introducing the velocity potentials

we obtain, using that the contribution from the pressure field vanishes

$$M_z = -\rho \int_{S_\infty} \overline{\frac{\partial \phi^{(1)}}{\partial \theta} \frac{\partial \phi^{(1)}}{\partial R}} dS - \rho U \int_{C_\infty} \overline{(y \frac{\partial \phi^{(1)}}{\partial R} - \frac{x}{R} \frac{\partial \phi^{(1)}}{\partial \theta}) \zeta^{(1)}} ds$$
$$- \rho U \int_{S_\infty} (y \frac{\partial \psi^{(2)}}{\partial R} - \frac{x}{R} \frac{\partial \psi^{(2)}}{\partial \theta}) dS + \rho U^2 \int_{C_\infty} y n_1 \overline{\zeta^{(2)}} ds \qquad (4)$$

where $R = (x^2 + y^2)^{1/2}$ is the radius of the cylinder, θ the polar angle, C_∞ denotes the water line of S_∞ and $\zeta^{(1)}$ and $\zeta^{(2)}$ are the first and second order free surface elevations, respectively. The formula (4) is valid for arbitrary U and water depth. We notice that the integrands in the two first terms are given by products of first order quantities. These terms are easily evaluated when the linear solution is known. The third term is, however, undetermined until the $\psi^{(2)}$-field is known. The last term will be neglected, being of $O(U^2)$.

2.2 The boundary value problem for $\psi^{(2)}$

The steady second order velocity enters in the expression (4) for M_z only multiplied with U. To leading order in the forward speed it is thus sufficient to consider the solution of $\psi^{(2)}$ for $U = 0$. $\psi^{(2)}$ then is determined by $\nabla^2 \psi^{(2)} = 0$ in the fluid, $\partial \psi^{(2)}/\partial n = 0$ on the wetted body surface, S_B, $\nabla \psi^{(2)} \to 0$ when $|\mathbf{x}| \to \infty$, and

$$\frac{\partial \psi^{(2)}}{\partial z} = -\frac{1}{g} \overline{\frac{\partial}{\partial t} \nabla \phi^{(1)} \cdot \nabla \phi^{(1)}} + \frac{1}{g^2} \overline{\frac{\partial \phi^{(1)}}{\partial t} \frac{\partial^3 \phi^{(1)}}{\partial z \partial t^2}} + \frac{1}{g} \overline{\frac{\partial \phi^{(1)}}{\partial t} \frac{\partial^2 \phi^{(1)}}{\partial z^2}} \quad \text{on } z = 0 \qquad (5)$$

The two first terms on the right hand side of (5) vanish since their time averages are identically zero. Introducing for the first order potential

$$\phi^{(1)} = Re(\phi e^{i\sigma t}) \qquad (6)$$

where σ denotes the frequency of encounter, the third term gives

$$\frac{\partial \psi^{(2)}}{\partial z} = -\frac{\sigma}{2g} Im(\phi \frac{\partial^2 \phi^*}{\partial z^2}) \quad \text{on } z = 0 \qquad (7)$$

where a star denotes complex conjungate. We note that $\partial \psi^{(2)}/\partial z$ for $z = 0$ generally is nonzero in the vicinity of the structure. However, $\partial \psi^{(2)}/\partial z = 0$ on the free surface in the far field. This is easily seen from (7) since ϕ is dominated by the wave part in the far field, i.e.

$$\phi(\mathbf{x}) = e^{Kz} \phi(x, y, 0) \qquad (8)$$

where K is the wave number. $Im(\phi \partial^2 \phi^*/\partial z^2)$ vanishes when (8) is satisfied. ϕ does, however, not satisfy (8) close to the structure, except in the special case when the structure is restrained and has vertical walls extending deeply in the fluid. In this case $Im(\phi \partial^2 \phi^*/\partial z^2) = 0$ on the entire free surface giving that the steady second order velocity disappears in the entire fluid domain. Thus, the $\psi^{(2)}$-field is generated by the presence of first order evanescent modes in near field of the structure, due to linear responses or non-vertical body boundaries. In practical applications we find that the $\psi^{(2)}$-field is significant when the linear motions of the structure are large, and that $\psi^{(2)}$ is small when the motions of the structure are small or the structure is restrained.

Since $\partial\psi^{(2)}/\partial z = 0$ on the free surface in the far field one can be lead to the conclusion that $\psi^{(2)}$ decays so rapidly when $R \to \infty$ that the third integral in (4) vanishes. This is, however, not true. It can be shown by applying Green's theorem to $\psi^{(2)}$ and a Green function satisfying the rigid wall condition at $z = 0$, that the far field behaviour of $\psi^{(2)}$ reads (see Grue and Palm 1992)

$$\psi^{(2)}(\mathbf{x}) = \frac{Q}{2\pi|\mathbf{x}|} + \mathbf{M}\cdot\nabla\frac{1}{2\pi|\mathbf{x}|} + ... \tag{9}$$

where

$$Q = \int_{S_F} \frac{\partial\psi^{(2)}}{\partial z} dS \tag{10}$$

$$\mathbf{M} = (M_1, M_2) = \int_{S_B} \psi^{(2)}\mathbf{n}_H dS - \int_{S_F} \frac{\partial\psi^{(2)}}{\partial z}\mathbf{x}_H dS \tag{11}$$

Here, $\mathbf{n}_H = (n_1, n_2, 0)$, $\mathbf{x}_H = (x, y, 0)$ and S_F denotes integration over the free surface. It can be shown that Q equals the Stokes' drift of opposite sign, i.e.

$$Q = -\int_{C_\infty} \overline{\zeta^{(1)}\frac{\partial\phi^{(1)}}{\partial n}} ds \tag{12}$$

Q equals zero when the structure is performing no work on the fluid.

2.3 The $\psi^{(2)}$-contribution to the moment

By substituting $\psi^{(2)}$ given by (9) into the third integral of (4) and carrying out the integration over S_∞, we obtain

$$-\rho U\int_{S_\infty}(y\frac{\partial\psi^{(2)}}{\partial R} - \frac{x}{R}\frac{\partial\psi^{(2)}}{\partial\theta})dS = -\rho U M_2 = -\rho U\int_{S_B}\psi^{(2)}n_2 dS + \rho U\int_{S_F} y\frac{\partial\psi^{(2)}}{\partial z}dS \tag{13}$$

This result can alternatively be shown more directly by application of Gauss' theorem and partial integration, without using the far field behaviour (9) of $\psi^{(2)}$, see Grue and Palm (1992). The integral in (13) over the body surface may be further transformed by introducing the function Ψ satisfying $\nabla^2\Psi = 0$ in the fluid, $\partial\Psi/\partial n = n_2$ on S_B, $\partial\Psi/\partial z = 0$ on S_F, and $\nabla\Psi \to 0$ when $|\mathbf{x}| \to \infty$. Ψ is the steady velocity potential if the body is moving along the positive y-axis (corresponding to χ when the body is moving along the positive x-axis). By applying Green's theorem to $\psi^{(2)}$ and Ψ and applying the boundary conditions on S_B and S_F it is easily shown that

$$\int_{S_B}\psi^{(2)}n_2 dS = \int_{S_F}\Psi\frac{\partial\psi^{(2)}}{\partial z}dS \tag{14}$$

Thus, the $\psi^{(2)}$-contribution to M_z reads

$$-\rho U\int_{S_\infty}(y\frac{\partial\psi^{(2)}}{\partial R} - \frac{x}{R}\frac{\partial\psi^{(2)}}{\partial\theta})dS = -\rho U\int_{S_F}\Psi\frac{\partial\psi^{(2)}}{\partial z}dS + \rho U\int_{S_F} y\frac{\partial\psi^{(2)}}{\partial z}dS \tag{15}$$

By (7) $\partial\psi^{(2)}/\partial z$ may be expressed in terms of the first order potential. Thus, the $\psi^{(2)}$-contribution to M_z is replaced by products of first order quantities. The integral over the free surface is easily evaluated numerically since $\partial\psi^{(2)}/\partial z$ decays rapidly with increasing distance from the body.

2.4 Complete expression for small U

The two first integrals of (4) may be further developed by introducing (6) for the first order potential. Furthermore, we decompose ϕ by

$$\phi = \frac{Aig}{\omega}(\phi_0 + \phi_B) \tag{16}$$

where A denotes the amplitude, ω the frequency and

$$\phi_0 = e^{Kz - iK(x\cos\beta + y\sin\beta)} \tag{17}$$

the potential of the incoming waves (for $U = 0$). The wave number is given by $K = \omega^2/g$, and the encounter frequency by $\sigma = \omega - UK\cos\beta$. β denotes the incidence angle, defined as the angle between the positive x-axis and the wave direction. $\beta = 0^0$ corresponds to following waves, and $\beta = 180^0$ to head waves. ϕ_B represents the sum of the diffraction and radiation potentials and is in the far field given by

$$\phi_B = R^{-1/2}H(\theta)e^{k_1(\theta)(z - iR\sqrt{1-4\tau^2\sin^2\theta})} + \mathcal{O}(\frac{1}{R}) \tag{18}$$

where $\tau = U\sigma/g$, $k_1 = \nu(1 + 2\tau\cos\theta) + o(\tau)$, $\nu = \sigma^2/g = K(1 - 2\tau\cos\beta) + o(\tau)$, and $H(\theta)$ is the amplitude distribution of the potential. Introducing this into (4) we obtain (see Grue and Palm 1992)

$$\begin{aligned}\frac{M_z}{\rho g A^2} = & - \frac{1}{4K}Im\{\int_0^{2\pi}(1 - 2\tau\cos\theta)H\frac{dH^*}{d\theta}d\theta\} - \frac{1}{2K}Im\{\frac{\nu}{K}S' + \tau\sin\beta S\} \\ & + \frac{\tau}{2K}\int_{S_F}(\Psi - y)Im[(\phi_0 + \phi_B)\frac{\partial^2}{\partial z^2}(\phi_0^* + \phi_B^*)]dxdy + o(\tau)\end{aligned} \tag{19}$$

where

$$\begin{aligned}S &= \sqrt{\frac{2\pi}{\nu}}e^{i\pi/4}H^*(\beta + 2\tau\sin\beta) \\ S' &= \sqrt{\frac{2\pi}{\nu}}e^{i\pi/4}(H'(\beta + 2\tau\sin\beta))^*\end{aligned} \tag{20}$$

and H' denotes derivative with respect to the argument. The first order motion for small forward speed is obtained by applying the method described by Nossen et al. (1991). There integral checks for the solution were developed and convergence of the method was discussed. The mean yaw moment is in the examples presented always obtained with an accuracy being better than 5%. Application of finer discretizations of the geometries will reduce this relative error. The evaluation of the free surface integrals is checked by computing the Stokes' drift by (10). This quantity should be zero in the examples where the structure is performing no work on the fluid, which is the case in the applications presented here. The computed values of Q is always found to be smaller than about 5 per mille of the Stokes' drift of the incoming waves per characteristic length of the marine structure.

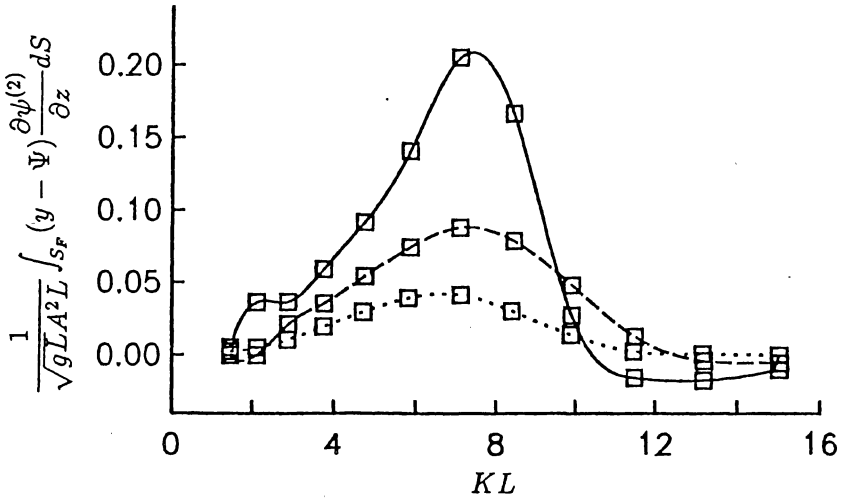

Figure 1: $\psi^{(2)}$-contribution to M_{z1} for the TPS vs. wave number. Solid line: $\beta = 100^0$, dashed line: $\beta = 140^0$, dotted line: $\beta = 160^0$. ($\beta = 180^0$ corresponds to head waves.)

3 The near field method

The second way to obtain the mean yaw moment is by applying direct pressure integration over the body. The fluid pressure is given by Bernoulli's equation which, keeping terms $O(U)$, reads

$$p = -\rho(\frac{\partial\Phi}{\partial t} + U\nabla\chi_s \cdot \nabla\Phi + \frac{1}{2}|\nabla\Phi|^2 + gz) + C(t) \tag{21}$$

where $C(t)$ is an arbitrary function of time, $\chi_s = -x + \chi$ and Φ is decomposed as in (2). All the terms in (21) (except $C(t)$) give rise to steady second order contributions due to the first order motions of the fluid and the structure. The term $-\rho U\nabla\chi_s \cdot \nabla\Phi$ contributes, however, also to the mean yaw moment by $-\rho U\int_{S_B}\nabla\chi_s \cdot \nabla\psi^{(2)}n_6 dS$ where $n_6 = \mathbf{k}\cdot(\mathbf{x}\times\mathbf{n})$. The solution for $\psi^{(2)}$ is then in principle needed to evaluate this integral. However, Grue and Palm (1992) show that this contribution may be expressed by the following integral over the free surface, i.e.

$$-\rho U\int_{S_B}\nabla\chi_s \cdot \nabla\psi^{(2)}n_6 dS = -\rho U\int_{S_F}\Psi\frac{\partial\psi^{(2)}}{\partial z}dS - \rho U\int_{S_F}\frac{\partial\psi^{(2)}}{\partial z}(x\frac{\partial\chi}{\partial y} - y\frac{\partial\chi}{\partial x})dS \tag{22}$$

Using (7), we obtain similarly as for the far field method, that also the $\psi^{(2)}$-contribution to the moment by the near field method can be determined without knowing the explicit solution for $\psi^{(2)}$. Instead we only need to integrate products of $\phi^{(1)}$-terms over the free surface. We note that the contributions from $\psi^{(2)}$ by the near field and far field methods are different. The first term on the right hand sides of (15) and (22) are identical. However, the second term of (15) differ from the second term of (22). These terms are always found to be very different in magnitude, with the former completely dominating the latter.

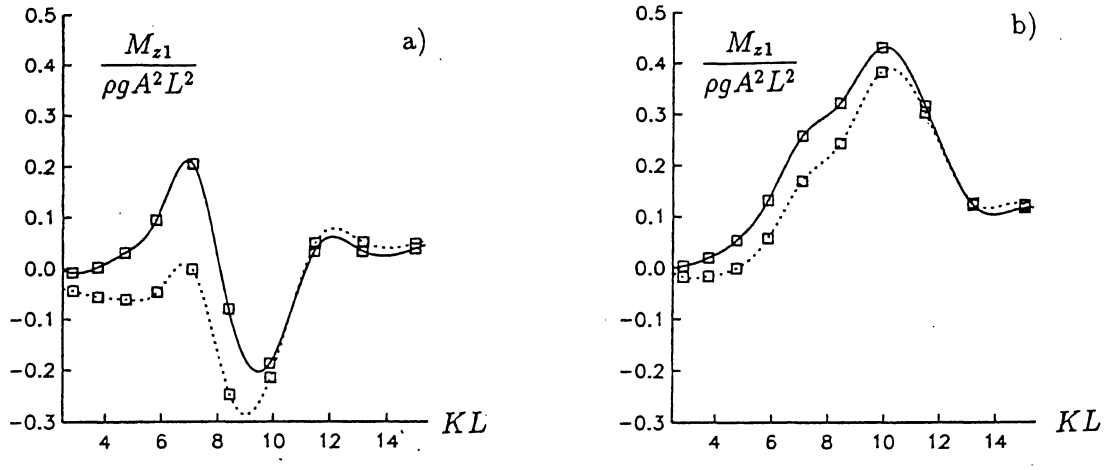

Figure 2: Forward speed part of the moment, M_{z1}, for the TPS vs. wave number. Solid line: Total value, with $\psi^{(2)}$ included. Dotted line: Without the $\psi^{(2)}$-contribution. a. $\beta = 100^0$, b. $\beta = 140^0$.

4 Numerical examples

4.1 The turret production ship

In the first examples we consider a turret production ship (TPS) with length $L = 230m$ and beam $B = 41m$. The ship is not moored. We evaluate M_z by the far field method, using (19). For small forward speed we may write the moment by

$$M_z = M_{z0} + FrM_{z1} + O(Fr^2) \tag{23}$$

where M_{z0} denotes the moment at $U = 0$, $Fr = U/\sqrt{gL}$ denotes the Froude number and FrM_{z1} gives the change in the moment due to U.

Our intention is to discuss the $\psi^{(2)}$-contribution to M_z and to give a total picture of M_z for small forward speed. Let us first consider the $\psi^{(2)}$-contribution which is obtained by evaluating (15). In figure 1 results are shown for $\beta = 100^0$, 140^0 and 160^0. We observe that the peak values of the curves, which are occurring close to resonance in heave and pitch, are for the three values of β approximately proportional to $180^0 - \beta$. The largest effect of $\psi^{(2)}$ is occurring for beam seas! At a first glance this is a surprising result. However, there is a very simple explanation for this feature.

First we remark that $\partial\psi^{(2)}/\partial z$ is always found to be large in magnitude (negative for the TPS) on the weather side of the structure and small on the lee side. Next we note that the Ψ-field is antisymmetric with respect to $y = 0$ when the marine structure is symmetric with respect to $y = 0$, i.e. $\Psi(x, y, z) = -\Psi(x, -y, z)$. This is true for the TPS. Close to head seas ($\beta = 180^0$) or following seas ($\beta = 0^0$), $\partial\psi^{(2)}/\partial z$ is approximately symmetric with respect to $y = 0$. When multiplied with the antisymmetric function $y - \Psi$ and integrated over the free surface, cancellation occurs. Close to beam seas, however, the main contribution to (15) comes from integrating $\partial\psi^{(2)}/\partial z$ multiplied with the weight function $y - \Psi$ over the free surface on the weather side of the ship. The variation of $\partial\psi^{(2)}/\partial z$ with respect to the x-coordinate is in this case

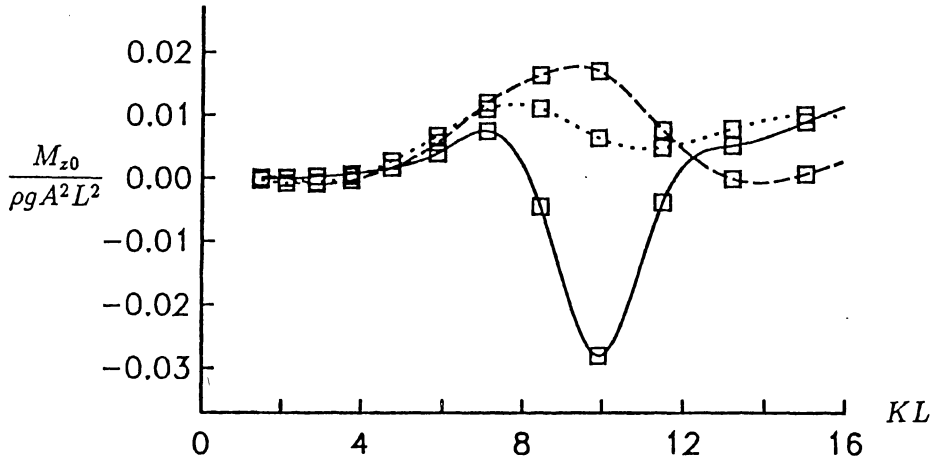

Figure 3: Mean yaw moment for $U = 0$, M_{z0}, for the TPS vs. wave number. Solid line: $\beta = 100^0$, dashed line: $\beta = 140^0$, dotted line: $\beta = 160^0$.

small. Thus, there is small cancellation along the ship's length direction, giving that large effect occurs.

The last term in the r.h.s. of (15) is in all examples with the TPS found to contribute with about two thirds of the total, while the first term contributes with the additional one third. If the near field method is used, the $\psi^{(2)}$-contribution is given by (22). The magnitude of (22) is in all examples here found to be about one third of (15), since the last term of (22) always is very small.

Next we consider the complete values of M_{z1} for the TPS compared to the values without the $\psi^{(2)}$-contribution, see figures 2a-b. We observe that the $\psi^{(2)}$-term is important for longer waves, i.e. for $KL < 10$. This corresponds to the wave period being larger than about $10s$ for which the wave spectrum very often has its maximal value.

Finally, we compare M_{z1} with the zero speed moment M_{z0} which is shown in figure 3. We observe that the non-dimensional values of M_{z1} is about 25 times larger than the corresponding values of M_{z0} for $\beta = 140^0$. This means that for $U = 2ms^{-1}$, i.e. $Fr \simeq 0.04$, the total moment experiences a 100% increase compared to zero speed. This result is also true for $\beta = 100^0$ and $KL < 8$. For $KL \simeq 9$, however, $U = 2ms^{-1}$ increases the magnitude of M_z with only 25%. M_z is then negative.

4.2 The tension-leg platform

In the next examples we consider a tension-leg platform (TLP). The submerged part is composed by four vertical circular columns, each of radius a and draught $3a$, placed on a ring-like pontoon with breadth $2a$, height $1.4a$ and outer diameter $11.9a$. The column centers generate a square with sides of length $7a$ being parallel to the x- and y-directions. In full scale examples we set the column radius $a = 10m$. It is relevant to assume for a TLP that the linear responses are only in surge and sway, and that the mass equals 75% of the displaced water mass. Again the moment is written in the form (23), where now the length scale in the Froude number is the column radius, i.e. $Fr = U/\sqrt{ga}$.

First we consider the $\psi^{(2)}$-contribution (15) to M_z by the far field method, with

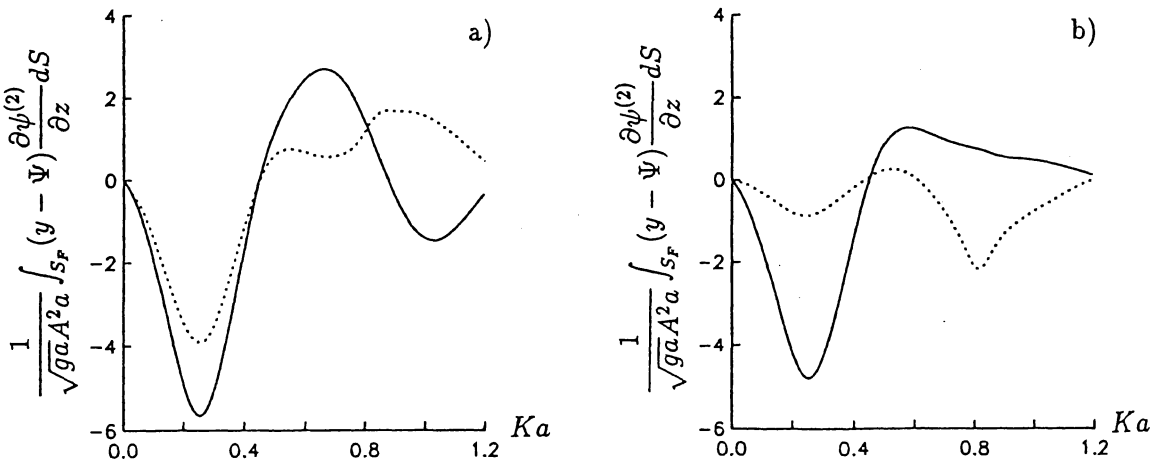

Figure 4: $\psi^{(2)}$-contribution to M_{z1} for the TLP vs. wave number. a. Solid line: $\beta = 90^0$, dotted line: $\beta = 135^0$. b. Solid line: $\beta = 120^0$, dotted line: $\beta = 170^0$.

results shown in figure 4. The computations show that about 95% of the total $\psi^{(2)}$-contribution to the moment now comes from the second term of (15), i.e. by integrating $y\partial\psi^{(2)}/\partial z$ over the free surface. This result is special for the platform geometry which is characterized by the distances between the columns being much larger than the column radius. $\partial\psi^{(2)}/\partial z$ is found to be nonzero only in the vicinity of the columns where we have that $|\Psi|/|y|$ varies from zero and up to about 0.3. This gives that the main contribution comes from $\int_{S_F} y\partial\psi^{(2)}/\partial z dS$, emphasizing again the antisymmetric nature of the $\psi^{(2)}$-contribution to the moment with respect to the forward speed direction. As a consequence the largest effect, as for the TPS, is obtained for $\beta = 90^0$ (see figure 4).

If direct pressure integration was applied in stead of the far field method, the $\psi^{(2)}$-contribution is given by (22). This term is very small for the TLP and can, in view of the remarks above, be neglected.

Results for the complete M_{z1} for the TLP has been shown earlier by Grue and Palm (1991 fig.8), however, without taking into account the effect of $\psi^{(2)}$. Here this contribution is included, and the results are shown in figures 5a-c. We observe that M_{z1} exhibits a strong variation with respect to the wave number. This is due to interference in the wave field generated by the different columns. The computations show that the effect of $\psi^{(2)}$ on M_{z1} is important when $Ka < 0.4$, which corresponds to wave periods being larger than $10s$ (for $a = 10m$). For non-dimensional wave numbers larger than 0.4 (and wave periods smaller than about $10s$) the effect of $\psi^{(2)}$ in evaluating M_{z1} can, practically speaking be disregarded, since the other terms then become dominating. This conclusion also holds for all values of Ka when β is close to 180^0.

The total steady yaw moment is obtained by adding M_{z0} and FrM_{z1}. Characteristic feature for $\beta = 90^0, 135^0$ is that M_{z0} equals zero due to symmetry, such that FrM_{z1} gives the total moment. The zero speed moment is, however, non-zero for $\beta = 120^0$, see figure 5d. We remark that M_{z0} like M_{z1} exhibits a strong variation with respect to the wave number. By comparing the results for M_{z1} (figure 5c) with the results for M_{z0} (figure 5d) we observe that the former is 5 to 10 times larger in magnitude than the latter. Thus, for $U = 1ms^{-1}$, which corresponds to a Froude number $Fr = U/\sqrt{ga} = 0.1$, the

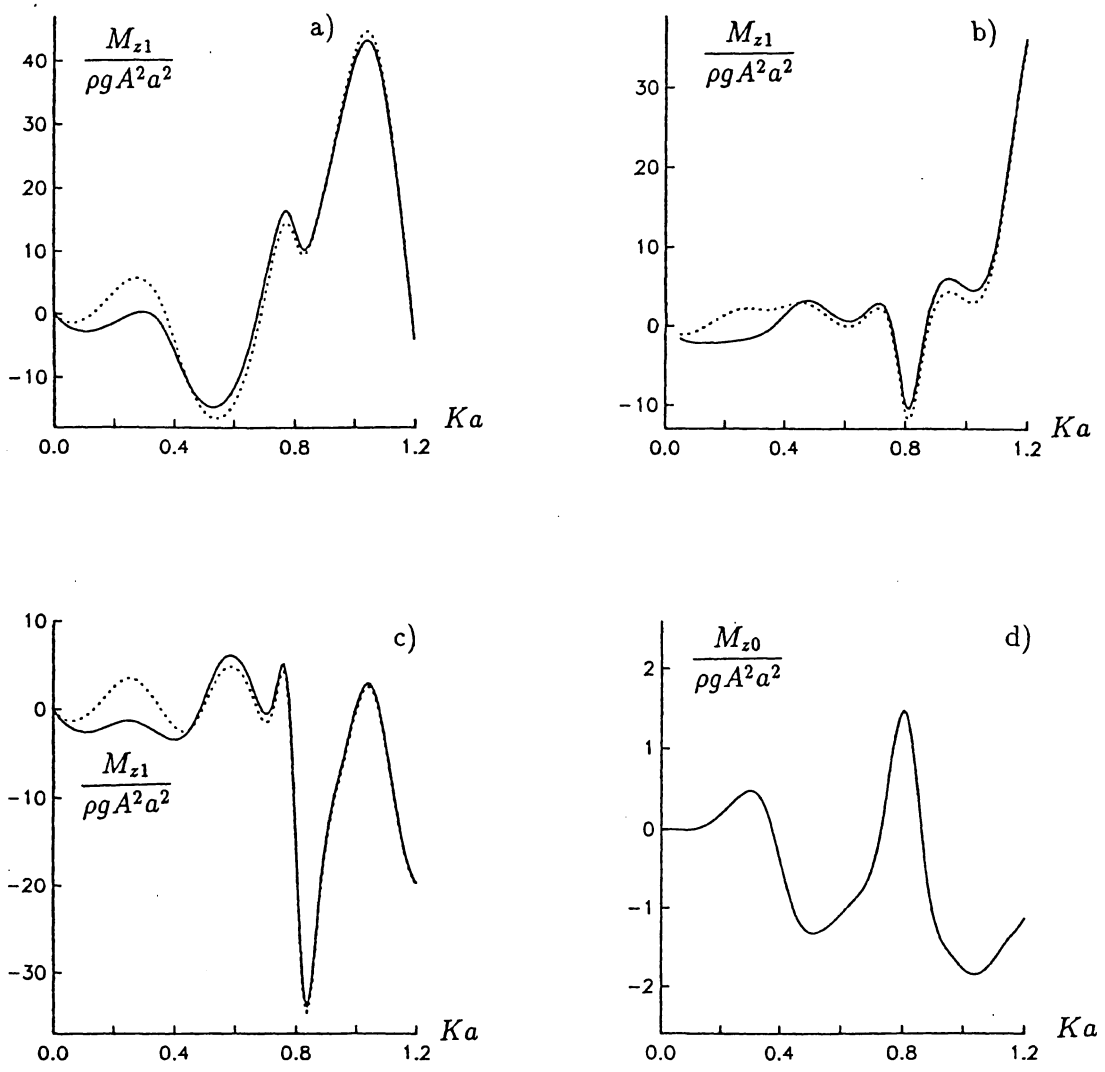

Figure 5: a.-c.: Forward speed part of the moment, M_{z1}, for the TLP vs. wave number. Solid line: Total value, with $\psi^{(2)}$ included. Dotted line: Without the $\psi^{(2)}$-contribution. a. $\beta = 90^0$, b. $\beta = 120^0$. c. $\beta = 135^0$. d. Mean yaw moment for $U = 0$, M_{z0}, for the TLP vs. wave number. $\beta = 120^0$.

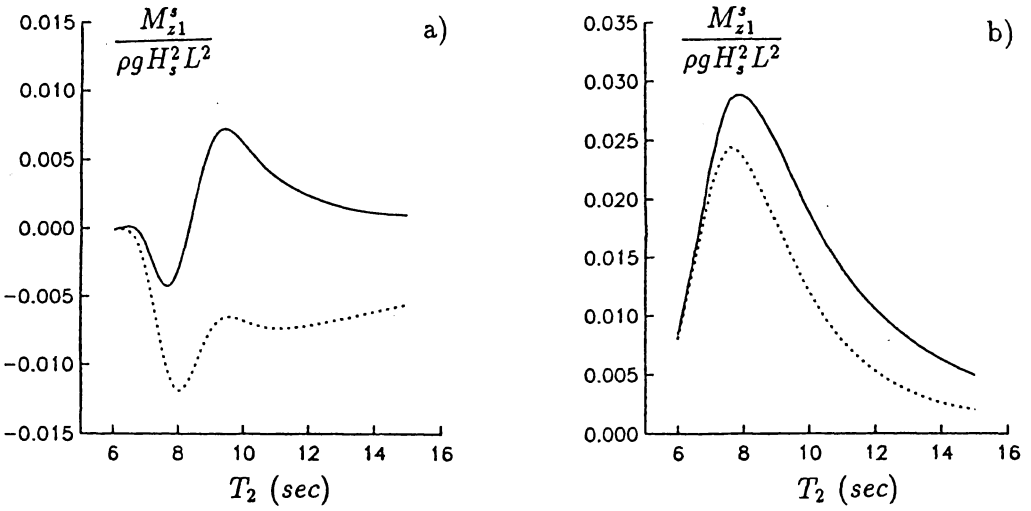

Figure 6: Forward speed part of the mean yaw moment, M^s_{z1}, for the TPS in irregular sea vs. mean wave period, T_2, of the spectrum. Solid line: Total value, with $\psi^{(2)}$ included. Dotted line: Without the $\psi^{(2)}$-contribution. a. $\beta = 100^0$. b. $\beta = 140^0$.

moment may be increased by 50 - 100% compared to $U = 0$.

4.3 Applications to irregular sea

To further illustrate the effect of the $\psi^{(2)}$-field we also evaluate the mean yaw moment due to an irregular sea. The waves are assumed to be long-crested and described by the JONSWAP spectrum. This spectrum depends on the mean wave period, T_2, and the significant wave height, H_s, see e.g. Faltinsen (1990, pp. 25-26). The mean yaw moment in the irregular sea is then given by

$$M^s_z = M^s_{z0} + FrM^s_{z1} + O(Fr^2) \tag{24}$$

where

$$M^s_{zk} = 2\int_0^\infty M_{zk} S(\omega) d\omega / A^2, \quad k = 0, 1 \tag{25}$$

and $S(\omega)$ denotes the wave spectrum. Results for M^s_{z1} as a function of the mean wave period T_2 are shown in figure 6 for the TPS. We note that $T_2 = 10s$ corresponds to a non-dimensional value $T_2\sqrt{g/L} = 2.06$, since $L = 230m$. The importance of the $\psi^{(2)}$-contribution is again emphasized. For $\beta = 100^0$ we note that completely wrong values of M^s_{z1} is obtained if $\psi^{(2)}$ is neglected. For $\beta = 140^0$, $\psi^{(2)}$ contributes with 30% to M^s_{z1} if the mean wave period is $10s$, and with 50% if the mean wave period exceeds $12s$.

Results for the mean yaw moment acting on the TLP in irregular seas are shown in figure 7. $T_2 = 10s$ corresponds to a non-dimensional value $T_2\sqrt{g/a} = 10$, since $a = 10m$. The computations show that M^s_{z1} are almost the same for $\beta = 90^0$ (figure 7a), $\beta = 120^0$ (figure 7b) and $\beta = 135^0$ (results not shown) when T_2 is larger than $8 - 9s$. Furthermore we remark that the the effect of $\psi^{(2)}$ becomes important when T_2 exceeds $8s$, and cannot be neglected. Finally we show results for the mean yaw moment on the TLP at zero speed and $\beta = 120^0$ (figure 7c). M^s_{z0} is a factor 10 smaller than M^s_{z1} when T_2 is in the range $5 - 8s$, and vanishes for larger T_2. As a consequence, the

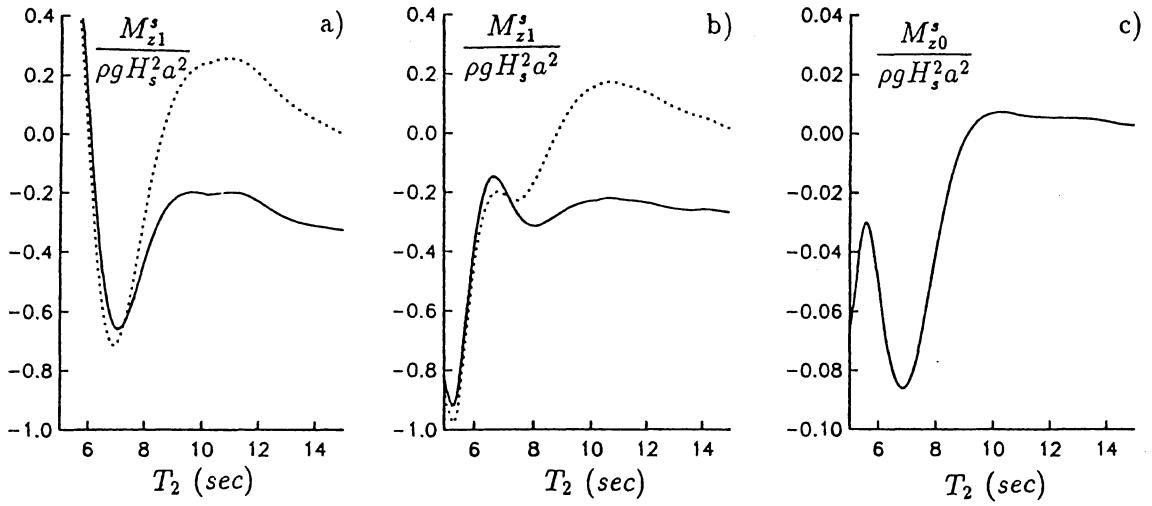

Figure 7: Mean yaw moment for the TLP in irregular sea vs. mean wave period, T_2, of the spectrum. a. M^s_{z1} for $\beta = 90^0$, and b. M^s_{z1} for $\beta = 120^0$. Solid line: Total value, with $\psi^{(2)}$ included. Dotted line: Without the $\psi^{(2)}$-contribution. c. M^s_{z0} for $\beta = 120^0$.

forward speed part of the moment gives the main contribution when the mean wave period exceeds $8 - 9s$. This result is independent of the wave angle.

5 Conclusions

The mean yaw moment, M_z, acting on a TPS or a TLP moving with forward speed in waves is discussed. A forward speed of $1 - 2ms^{-1}$ may increase M_z by 100% compared to $U = 0$. Special emphasis is given to the effect of the steady second order velocities, the $\psi^{(2)}$-field, which enter in the expressions for M_z multiplied by U. When the far field method is used, $\psi^{(2)}$ is found to contribute with 30-100% to the forward speed part of M_z when the wave period is larger than $9 - 10s$. For shorter waves the effect of $\psi^{(2)}$ may be neglected. When the near field method is applied, $\psi^{(2)}$ contributes with up to about 15% to the forward speed part of M_z for the TPS. $\psi^{(2)}$ can be neglected when the near field method is used to evaluate M_z for the TLP.

References

[1] FALTINSEN, O. M., 1990, Sea loads on ships and offshore structures. *Cambridge Univ. Press*

[2] GRUE, J. AND PALM, E., 1991, Currents and wave forces on ships and marine structures. In: *Dynamics of marine vehicles and structures in waves.* Eds. W. G. Price, P. Temarel and A. J. Keane, Elsevier

[3] GRUE, J. AND PALM, E., 1992, The mean drift force and yaw moment on marine structures in waves and current. *Submitted*

[4] NOSSEN, J., GRUE, J. AND PALM, E., 1991, Wave forces on three-dimensional floating bodies with small forward speed. *J. Fluid Mech.* **227**, 135-160.